A compressible LES with immersed boundary method

A. M. Akbarzadeh*, and I. Borazjani†
J. Mike Walker '66 Department of Mechanical engineering, Texas A&M University, College Station, TX, 77840

A subgrid-scale model for compressible flows suitable for the sharp-interface immersed boundary method is developed to perform large-eddy simulation (LES) of compressible flows involving turbulent flows, shock waves, and immersed bodies. The inviscid fluxes of compressible flow equations in curvilinear coordinates are discretized with a hybrid discretization comprising a fourth-order central scheme and a third-order weighted essentially non-oscillatory (WENO) scheme. The method is validated for two studies. In the first study, the LES model and numerical scheme are validated for decaying isotropic turbulent flow with Mach number $M_t = 0.4$. Afterwards, they are validated for a moving shock interacting with a cylinder. The results of simulations reveal that LES can properly resolve the inertial subrange and the hybrid scheme can capture shocks.

I. Introduction

Large eddy simulation (LES) is widely used for modeling turbulent compressible flows [1, 2]. In LES modeling, large-scale flow is computed by solving filtered Navier-Stokes equations and the effect of small-scale flow on the large-scale flow is modeled. One of the main challenges in LES of compressible flows is modeling shock turbulence interaction because it requires special schemes to accurately capture shock waves as well as resolve turbulent fluctuations. The weighted essentially non-oscillatory (WENO) schemes [3, 4] have been used intensively to capture shocks as they are accurate and robust at the same time [5]. However, WENO schemes are dissipative and are not suitable for LES modeling because their dissipative nature may dominate the dissipation from the subgrid-scale modeling. Non-dissipative schemes such as a central or compact scheme are typically used in LES to have the subgrid-scale modeling as the only source of dissipation. To treat this problem, hybrid schemes [6, 7] are developed which have a non-oscillatory scheme such as WENO near the shock and a non-dissipative scheme such as a central or compact

*PhD candidate, J. Mike Walker '66 Department of Mechanical engineering, Texas A& M University, College Station, TX
†Associate Professor, J. Mike Walker '66 Department of Mechanical engineering, Texas A& M University, College Station, TX

scheme far from the shock. The transition between schemes is typically performed by switch functions which have been studied extensively in previous studies [7, 8].

Shock turbulence interaction is a complex flow that is observed in transonic/supersonic flows, e.g., flow in high speed rotors and supersonic aircrafts, where both have moving surfaces with complex geometries. In fact, the presence of a moving or complex geometry in shock turbulent flows adds more complexity to the flow. To handle shock turbulent flows involving complex geometries, immersed boundary method along with a low order hybrid scheme such as fourth order central and third order WENO can be a suitable option because: i) immersed boundary methods (IBM) can handle arbitrarily large deformation and complex geometries properly [9], ii) third order WENO along with IBM can handle shock capturing [10, 11], and iii) capability of a hybrid third order WENO and central schemes for LES modeling have been confirmed [8]. In fact, a third order WENO and a central scheme has a small stencil (3 to 5, for second order and fourth order central schemes, respectively), which reduces the computational cost and alleviates the numerical implementation near the immersed boundary.

In this study, a compressible LES immersed boundary method with a hybrid scheme (third order WENO and central) is developed to model turbulence-shock interaction involving moving solid particles and complex geometries. First, LES will be validated against DNS result by simulations of decaying isotropic turbulent flow, which is a key turbulent feature for calibrating phenomenological turbulence models. Afterwards, we investigate the capability of our hybrid scheme immersed boundary framework for shock capturing by performing 2D simulations of the diffraction of a moving shock by a circular cylinder. The rest of this manuscript is organized as follows. In §II the governing equations, LES modeling, and numerical method for solving the flow is illustrated. The results of turbulence decay and shock diffraction by cylinder are shown in §III. Finally, the conclusion and future work will be presented in §IV.

II. method

To date, subgrid-scale models have been used extensively to model turbulent flows in different turbulent regimes such as isotropic turbulent flows [12–14], wall flows [15, 16], and shock wave turbulence interaction [17, 18]. The LES model of this study is employed based on subgrid-scale models of Moin et al. [2], which is similar to its incompressible version [15]. This LES model in conjunction with our immersed boundary method [9, 19–21] has been validated extensively in our incompressible framework [22, 23] and, been utilized in different applications such as flow control [24], vortex flows [25], and fish locomotion [26]. The detail of implementation of the compressible subgrid-scale model

in our framework is explained as follows.

The governing equations for the filtered compressible flow in curvilinear coordinates $\xi^q (m, p, q, r = 1, 2, 3$ and repeated indices imply summation) are as follows:

$$\frac{1}{J}\frac{\partial \mathbf{Q}}{t} + \frac{\partial}{\partial \xi^q}(\mathbf{F}^q - \mathbf{F}_v^q) = \mathbf{G}, \tag{1}$$

where Q is the variable vector, $\mathbf{F^q}$ and $\mathbf{F_v^q}$ are the filtered inviscid and viscous flux vectors, respectively:

$$Q = \begin{bmatrix} \bar{\rho} \\ \bar{\rho}\tilde{u}_1 \\ \bar{\rho}\tilde{u}_2 \\ \bar{\rho}\tilde{u}_3 \\ \bar{\rho}\tilde{E} \end{bmatrix} \mathbf{F}^q = \frac{1}{J}\begin{bmatrix} \bar{\rho}\tilde{U}^q \\ \bar{\rho}\tilde{u}_1\tilde{U}^q + \xi^q_{x_1}\bar{p} \\ \bar{\rho}\tilde{u}_2\tilde{U}^q + \xi^q_{x_2}\bar{p} \\ \bar{\rho}\tilde{u}_3\tilde{U}^q + \xi^q_{x_3}\bar{p} \\ (\bar{\rho}\tilde{E} + \bar{p})\tilde{U}^q \end{bmatrix} \mathbf{F}_v^q = \frac{1}{J}\begin{bmatrix} 0 \\ \xi^q_{x_r}(\tilde{\sigma}_{1r} - \tau_{1r}) \\ \xi^q_{x_r}(\tilde{\sigma}_{2r} - \tau_{2r}) \\ \xi^q_{x_r}(\tilde{\sigma}_{3r} - \tau_{3r}) \\ \xi^q_{x_r}(\tilde{K}_r) \end{bmatrix} G = \begin{bmatrix} 0 \\ 0 \\ 0 \\ 0 \\ -\alpha - \beta - \pi + \epsilon \end{bmatrix} \tag{2}$$

where the overbar denotes a filter operation, which commutes with the partial derivatives. The tilde filter represents the Favre filter operation, which is defined as $\tilde{u} = \overline{\rho u}/\bar{\rho}$, where ρ is density, $\tilde{u}_p$ $(p = 1, 2, 3)$ is the p^{th} component of the filtered Cartesian velocity, E is the total energy per unit mass, $J = |\partial(\xi^1, \xi^2, \xi^3)/\partial(x_1, x_2, x_3)|$ is the determinant of the Jacobian of the transformation, $\xi^q_{x_r}$, $\tilde{U}^q = \tilde{u}_r\xi^q_{x_r}$ is the contravariant velocity, $\tilde{p} = (\gamma - 1)(\bar{\rho}E - 0.5\bar{\rho}\tilde{u}_r\tilde{u}_r)$ is filtered pressure, γ is the ratio of the specicic heats, $\tilde{\sigma}_{rm} = \bar{\mu}(\xi^p_{x_m}\frac{\partial \tilde{u}_r}{\partial \xi^p} + \xi^p_{x_r}\frac{\partial \tilde{u}_m}{\partial \xi^p}) - \frac{2}{3}\mu\xi^p_{x_k}\frac{\partial \tilde{u}_k}{\partial \xi^p}\delta_{rm}$ is the filtered shear stress tensor in curvilinear coordinates, μ is the dynamic viscosity, δ_{rm} is the Kronecker delta tensor, $K_r = \gamma\mu Pr^{-1}\xi^p_{x_r}\partial(E - \frac{1}{2}\tilde{u}_m\tilde{u}_m)/\partial\xi^p + \tilde{u}_p\tilde{\sigma}_{rp}$, Pr is the Prandtl number. Here, τ_{rm} is the subgrid stress tensor (SGS) of the momentum equation. Based on the model proposed by Vreman et al. [27], the subgrid-terms in the energy equations have the following form in Cartesian coordinates:

$$\begin{aligned} \alpha &= \tilde{u}_i\partial_j(\bar{\rho}\tau_{ij}) \\ \beta &= \partial_j(\overline{pu_j} - \bar{p}\tilde{u}_j)(\gamma - 1) \\ \pi &= \overline{p\partial_j u_j} - \bar{p}\partial_j\tilde{u}_j \\ \epsilon &= \overline{\sigma ij\partial_j u_i} - \bar{\sigma}_{ij}\partial_j\tilde{u}_i, \end{aligned} \tag{3}$$

where α is the turbulent stress term on the scalar level. β is the pressure-velocity subgrid-term, π is the pressure-dilatation and ϵ is subgrid-scale turbulent dissipation. The SGS term (τ_{ij}) is modeled using model proposed by Moin et al.[2] as follows:

$$\tau_{ij} = \frac{2}{3} C_I \bar{\rho} \Delta^2 |\tilde{S}|^2 \delta_{ij} - 2 C_s \bar{\rho} \Delta^2 |\tilde{S}| (\tilde{S}_{ij} - \frac{1}{3} \tilde{S}_{mm} \delta_{ij}), \tag{4}$$

where the first term is the isotropic term of the SGS and the second term is the eddy viscosity term. Here, C_s is the Smagorinsky constant that can be modeled dynamically [2] or be a constant value ($C_s = 0.01$) similar to the values used for incompressible flows. However, the term C_I can be modeled dynamically [2] or assumed to be zero ($C_I = 0$) [27] due to instability problems. For modeling subgrid terms of the energy equations ($\alpha, \beta, \pi, \epsilon$), a similarity model proposed by Vreman et al.[27] is applied.

Here, the viscous terms are discretized with a second order central scheme, and the convective terms are discretized by a hybrid WENO-central scheme. The hybridization is applied using a switch function that smoothly transform from a fourth order central scheme to a third order WENO scheme [4] in the vicinity of the shock by a switch function proposed by Wu and Zhao [8]. The detail of the discretization of the convective flux is described for the 1D version ($q = 1$) of eqn. 1 for simplicity as follows:

$$\frac{\partial \mathbf{F}_i}{\partial \xi} = \left(\frac{\hat{\mathbf{F}}_{i+1/2} - \hat{\mathbf{F}}_{i-1/2}}{\Delta \xi} \right), \tag{5}$$

where i denotes cell center location, and $i \pm 1/2$ denotes cell interface location, where the fluxes are computed. The flux $\mathbf{F_{i+1/2}}$ in a hybrid scheme is

$$\hat{\mathbf{F}}_{i+1/2} = \sigma_{i+1/2} \mathbf{F}^{central}_{i+1/2} + (1 - \sigma_{i+1/2}) \mathbf{F}^{WENO}_{i+1/2} \tag{6}$$

where $\sigma_{i+1/2}$ is the switch function, $\mathbf{F}^{central}_{i+1/2}$ and $\mathbf{F}^{WENO}_{i+1/2}$ are the central and WENO fluxes, respectively. Here, $\mathbf{F}^{central}_{i+1/2}$ is calculated from the exact equation 1 by using ($\mathbf{Q_{i+1/2}}$) that is obtained from a fourth-order central interpolation, e.g., $Q_{i+1/2} = -1/6 Q_{i-1} + 4/6 Q_{i-1} + 4/6 Q_{i+1} - 1/6 Q_{i+2}$. The details of computing third-order WENO fluxes can be found in the previous study [4]. Herein, the $\sigma_{i+1/2}$ is obtained using the switch function proposed by Wu and Zhao [8] as follows:

$$\sigma_{i+1/2} = \frac{1}{2} \frac{tanh(\frac{3(r_{i+1/2} - r_d)}{max(r_d, |r_{i+1/2} - r_d|)})}{tanh(3)} + \frac{1}{2}, \tag{7}$$

where $r_{i+1/2} = min(r_i, r_{i+1})$, and r_i is obtained as follows:

$$r_i = \frac{|2\Delta f_{i+1/2}\Delta f_{i-1/2}| + \epsilon}{(\Delta f_{i+1/2})^2 + (\Delta f_{i-1/2})^2 + \epsilon}, \tag{8}$$

where $\Delta f_{i+1/2} = f_{i+1} - f_i$, $\epsilon < 10^{-10}$ is a small number to avoid divide by zero.

Finally, the governing equations are advanced in time using a third order Runge-Kutta method at each grid point similar to the immersed boundary method for compressible flows (without turbulence) [19]. The 3D, arbitrarily complex moving boundaries inside the domain are handled with a sharp-interface immersed boundary method [19] used previously for incompressible flows [28]. The grid nodes inside the immersed boundary (solid nodes) are blanked out, while the velocity on the nodes that are exterior to, but adjacent to, the immersed boundary (IB nodes) are reconstructed using an interpolation along the normal to the boundary [19, 28]. The background grid nodes are classified into solid, fluid and IB nodes by an efficient ray-tracing algorithm [9].

Note that the 3^{rd} order accuracy of the WENO and 4^{th} of the central scheme is only obtained on uniform grids. For non-uniform grids the order of accuracy of this discretization will be 2^{nd} order due to the 2^{nd} order accurate calculation of the metric of the transformation $\xi^q_{x_r}$.

III. Results

In this section, the validation studies performed for a turbulent compressible flow and shock interactions with an immersed boundary are presented.

A. decaying isotropic turbulent flow

To validate our computational scheme and our LES, large eddy simulations of isotropic decaying turbulence are performed with a dynamic C_s and the results are compared against the results of direct numerical simulations (DNS) of Samtaney et al. [12] and LES of Li et al. [10]. The computational details of this simulation are described as follows.

The computational domain is a cube of $[0, 2\pi] \times [0, 2\pi] \times [0, 2\pi]$ which is discretized evenly with 64 grid points in each direction. The boundary conditions are periodic for every parameter at all boundaries. Here, the Mach number is $M_t = u'/c = 0.4$, where u' is the turbulent fluctuation velocity and c is the speed of sound. The Reynolds number is $Re_\lambda = \lambda u'\rho/\mu = 153$, defined based on u' and taylor length scale (λ). The turbulence fluctuation velocity is $<u_i^2/3>$,

where <> is the volume average in the computational domain, u_i ($i = 1, 2, 3$) is the i-th component of the velocity vector, and Taylor length scale is defined as

$$\lambda^2 = \frac{u'^2}{< (\partial u_i/\partial x_i)^2 >}, \tag{9}$$

The simulation is initialized with a specified spectrum [12] for velocity which is divergence free initially and given by

$$E(k) = Ak^4 exp(-2k^2/k_0^2) \tag{10}$$

where k is the wave number, $k_0 = 6$ is the wave number at which the spectrum peaks, similar to study of Li et al. [10], and A is a constant chosen to get initial kinetic energy of 1.0. The turbulence decay is presented for different times (t/τ), where τ is the initial large-eddy turnover time, defined as

$$\tau = \sqrt{\frac{32}{A}}(2\pi)^{\frac{1}{4}} k_0^{\frac{-7}{2}} \tag{11}$$

The turbulence decay is presented in Fig. 1, which visualizes the magnitude of vorticity in computational domain at three different times $t/\tau = 1$, $t/\tau = 2$, and $t/\tau = 5$. The reduction of the magnitude of vorticity in time indicate the reduction of turbulence intensity of the flow. The plot of turbulent kinetic energy spectrum ($E(k)$) versus k is presented at 4 different times in Fig.1d. The computed plot for energy cascade at $t/\tau = 5$ reveals that the LES model can capture the inertial subrange as the energy spectrum follows the theoretical 5/3 power law. The validation of the study is performed by comparing the time history of turbulent kinetic energy (TKE) of the domain obtained from LES and DNS of Samtaney et al. [12] and LES of Li et al.[10] in Fig. 1e. The TKE is defined as TKE=$0.5 < u_i^2 >$. The plot for the time history of the TKE is in good agreement with the DNS at times $t/\tau > 2$, but there is a small discrepancy at $t/\tau < 2$, which can be due to lower grid resolution compared to DNS because a similar discrepancy is also observed in LES of Li et al. [10] which had a similar grid resolution. Nevertheless, the good agreement between the history of the turbulence decay of our simulations and previous studies [10, 12] show that our LES deployed and hybrid scheme can properly model the subgrid stress tensor.

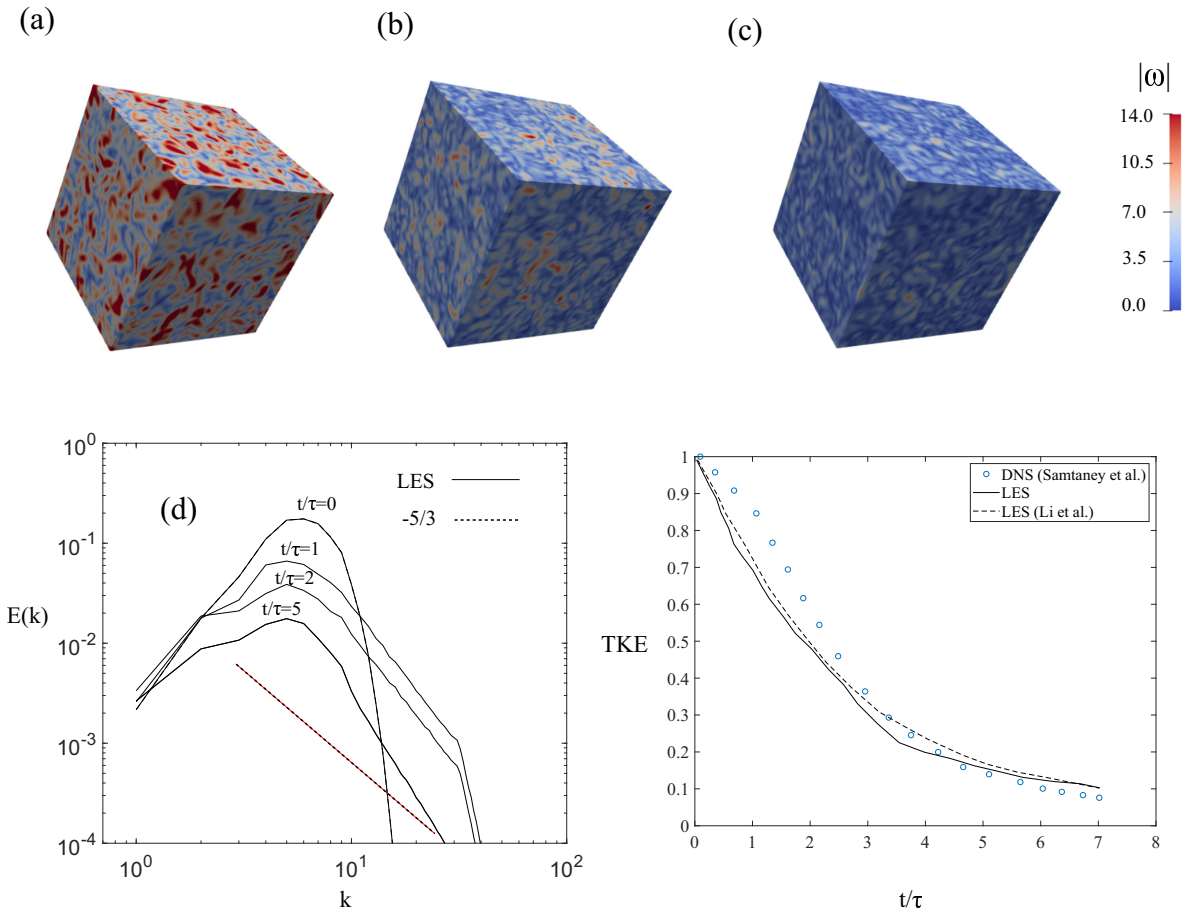

Fig. 1 (a) The decay of vorticity at (a) $t/\tau = 1$, (b) $t/\tau = 2$, and (c) $t/\tau = 5$. (d) The decay of energy spectrum $E(k)$ in time, (e) the decay of turbulence kinetic energy (TKE)

B. Shock diffraction

In this section, 2D simulation of the diffraction of a moving planar shock at Mach number M=2.81 with a stationary cylinder are presented. The simulations are performed with a hybrid scheme and C_s is 0.01. The domain size of the simulations is $25D \times 10D$, where D is the diameter of the cylinder, and meshed evenly with 4400×1200 nodes. The time-step is chosen $0.001D/U$ that corresponds to Courant–Friedrichs–Lewy (CFL) number of 0.2. The simulation is carried out with no-slip conditions on the surface of the cylinder. The Reynolds number $UD\rho/\mu = 8700$ (where $U = \sqrt{(p/\rho)}$ is the velocity scale, and μ is the dynamic viscosity behind the undisturbed shock) which matches the Reynolds number of experiments of Bryson and Gross [29]. Figure 2 shows the interaction of a moving shock with a cylinder. The moving shock is reflected by the cylinder (Fig. 2b) and generates a reflected shock (R.S.), incident shock (I.S.), and a Mach shock (M.S.). The intersection of the R.S., M.S.1, and I.S. is called the first triple point (T.P.1). The interaction of M.S.1 from the top and the bottom of the symmetry plane creates M.S.2 and their intersection creates

T.P.2 (Fig.2d). The contact discontinuity (C.D.2) is formed behind M.S.1 and M.S.2.

Figure 3a presents the comparison of the loci of the triple points, i.e., $x = 0$ and $y = 0$ corresponds to the center of the cylinder. As it can be observed in Fig. 2c, two triple points appear on either side of the plane of symmetry of the flow. The first one (T.P.1) starts at the front of the cylinder ($x/D = 0.0$), and the second one (T.P.2) at the plane of symmetry behind the cylinder ($x/D = 1.6$). The location of both triple point obtained from the simulation is in good agreement with the experimental results [29], which reveal that hybrid scheme and switch function can properly capture the shock waves for flows involving with immersed boundaries. Moreover, the flow is visualized with the contours of out-of-plane vorticity (ω_z) in Fig. 3b. The flow visualization shows vortex shedding in the wake of the cylinder at about 8.6D upstream of the moving shock. The shedding occurs when the shear layer in the wake of the cylinder becomes unstable.

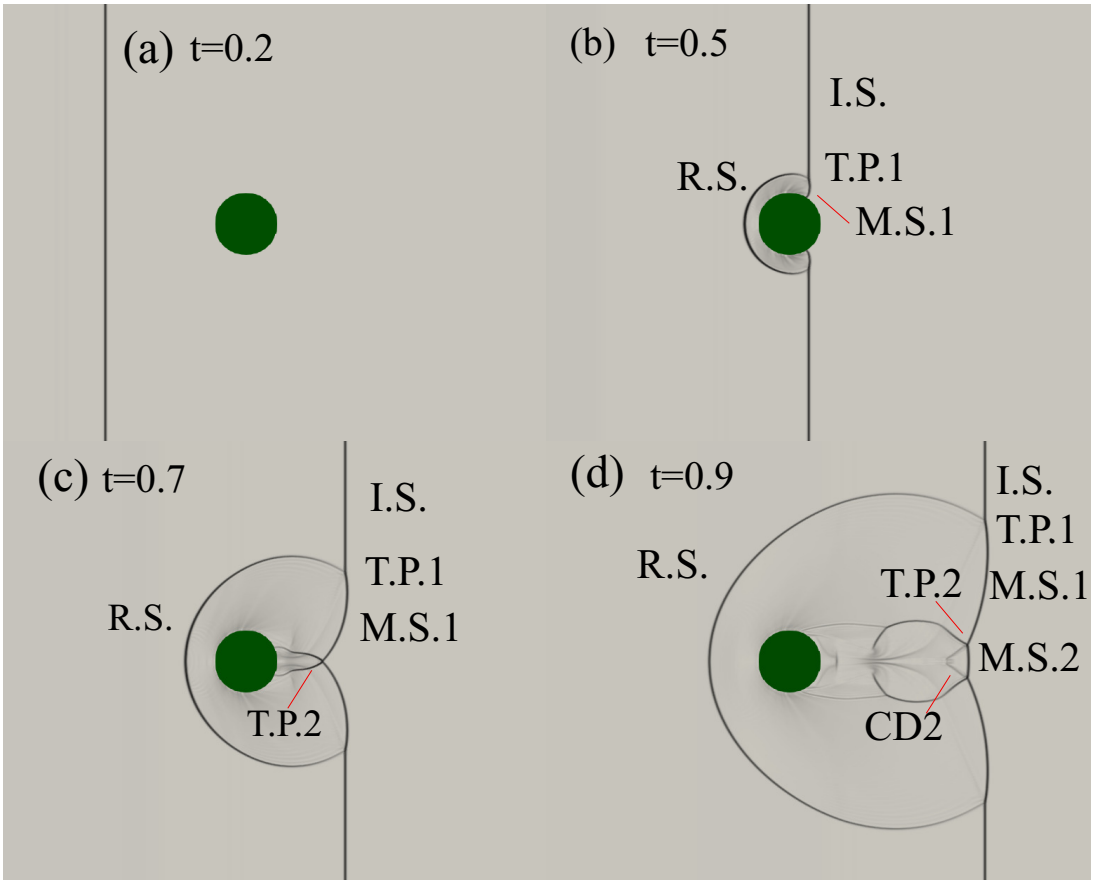

Fig. 2 The interaction of a moving shock and a circular cylinder. R.S. reflected shock, M.S.1 Mach shock, I.S. incident shock, T.P.1 the first triple point, and T.P.2 is the second triple point.

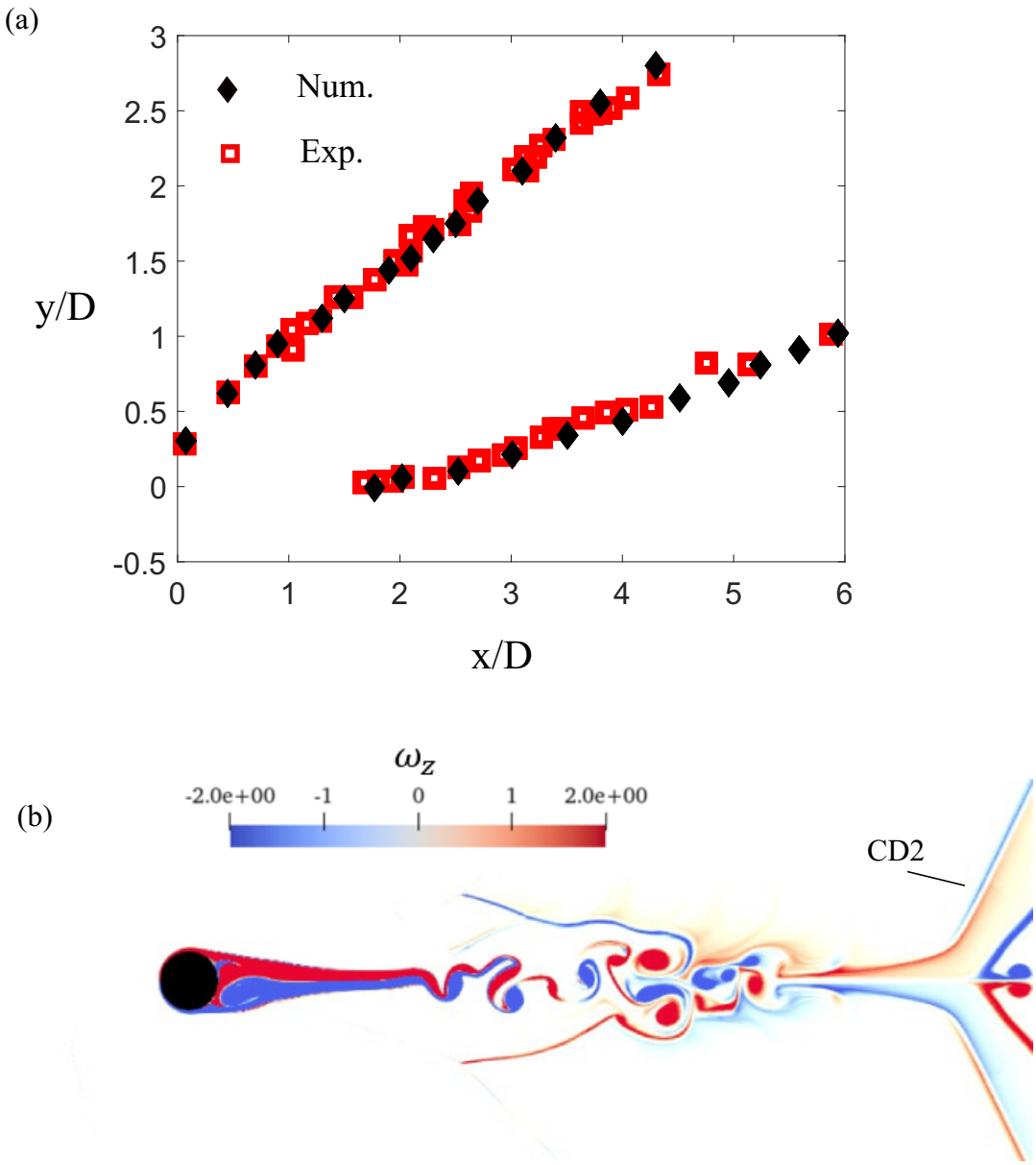

Fig. 3 (a) The location of the T.P.1 (upper curve) and T.P.2 from the simulation (Num.) and experimental results of Bryson and Gross [29]. (b) Contours of the vorticity in the wake of the cylinder at $t = 2.7$**.**

IV. Conclusions and Future work

A subgrid-scale LES for immersed boundary method is developed for modeling turbulent compressible flows involving immersed bodies. A hybrid fourth-order central and third-order WENO scheme along with a switch function are developed to handle shock turbulence interaction. The LES and numerical scheme are tested for a decaying isotropic turbulent flow and shock diffraction by a cylinder. It has been shown that the LES can properly resolve the inertial subrange and predict the turbulence decay for an isotropic turbulent flow with $Re_\tau = 153$ and Mach number of $M_t = 0.4$.

The simulations of shock diffraction by a cylinder are performed for a flow with $M = 2.81$ and $Re_D = 8700$. It has been presented that the switch function can properly handle the shock capturing by accurately predicting the position of the triple points. As a future work, the interaction of an incident shock in a channel with a turbulent boundary layer will be studied to validate the framework for turbulent-shock wave interaction.

Acknowledgments

This work was supported by the National Science Foundation (NSF) career grant CBET 1453982. The computational resources were partly provided by the High Performance Research Computing (HPRC) facilities at Texas A&M University.

References

[1] Garnier, E., Sagaut, P., and Deville, M., "Large eddy simulation of shock/boundary-layer interaction," *AIAA journal*, Vol. 40, No. 10, 2002, pp. 1935–1944.

[2] Moin, P., Squires, K., Cabot, W., and Lee, S., "A dynamic subgrid-scale model for compressible turbulence and scalar transport," *Physics of Fluids A: Fluid Dynamics*, Vol. 3, No. 11, 1991, pp. 2746–2757.

[3] Levy, D., Puppo, G., and Russo, G., "Central WENO schemes for hyperbolic systems of conservation laws," *ESAIM: Mathematical Modelling and Numerical Analysis*, Vol. 33, No. 3, 1999, pp. 547–571.

[4] Shu, C.-W., "Essentially non-oscillatory and weighted essentially non-oscillatory schemes for hyperbolic conservation laws," *Advanced numerical approximation of nonlinear hyperbolic equations*, Springer, 1998, pp. 325–432.

[5] Pirozzoli, S., "Numerical methods for high-speed flows," *Annual review of fluid mechanics*, Vol. 43, 2011, pp. 163–194.

[6] Lee, S., Lele, S. K., and Moin, P., "Eddy shocklets in decaying compressible turbulence," *Physics of Fluids A: Fluid Dynamics*, Vol. 3, No. 4, 1991, pp. 657–664.

[7] Pirozzoli, S., "Conservative hybrid compact-WENO schemes for shock-turbulence interaction," *Journal of Computational Physics*, Vol. 178, No. 1, 2002, pp. 81–117.

[8] Xiaoshuai, W., and Yuxin, Z., "A high-resolution hybrid scheme for hyperbolic conservation laws," *International Journal for Numerical Methods in Fluids*, Vol. 78, No. 3, 2015, pp. 162–187.

[9] Borazjani, I., Ge, L., and Sotiropoulos, F., "Curvilinear immersed boundary method for simulating fluid structure interaction with complex 3D rigid bodies," *Journal of Computational physics*, Vol. 227, No. 16, 2008, pp. 7587–7620.

[10] Li, Z., Ju, Y., and Zhang, C., "Hybrid central–WENO scheme for the large eddy simulation of turbulent flows with shocks," *Numerical Heat Transfer, Part B: Fundamentals*, Vol. 72, No. 2, 2017, pp. 170–189.

[11] Ghias, R., Mittal, R., and Dong, H., "A sharp interface immersed boundary method for compressible viscous flows," *Journal of Computational Physics*, Vol. 225, No. 1, 2007, pp. 528–553.

[12] Samtaney, R., Pullin, D. I., and Kosović, B., "Direct numerical simulation of decaying compressible turbulence and shocklet statistics," *Physics of Fluids*, Vol. 13, No. 5, 2001, pp. 1415–1430.

[13] Samiee, M., Akhavan-Safaei, A., and Zayernouri, M., "A fractional subgrid-scale model for turbulent flows: Theoretical formulation and a priori study," *Physics of Fluids*, Vol. 32, No. 5, 2020, p. 055102. https://doi.org/10.1063/1.5128379.

[14] Akhavan-Safaei, A., Seyedi, S. H., and Zayernouri, M., "Anomalous features in internal cylinder flow instabilities subject to uncertain rotational effects," *Physics of Fluids*, Vol. 32, No. 9, 2020, p. 094107. https://doi.org/10.1063/5.0021815.

[15] Germano, M., Piomelli, U., Moin, P., and Cabot, W. H., "A dynamic subgrid-scale eddy viscosity model," *Physics of Fluids A: Fluid Dynamics (1989-1993)*, Vol. 3, No. 7, 1991, pp. 1760–1765.

[16] Jahromi, R., Rezaei, M., Samadi, S. H., and Jahromi, H., "Biomass gasification in a downdraft fixed-bed gasifier: Optimization of operating conditions," *Chemical Engineering Science*, 2020, p. 116249. https://doi.org/10.1016/j.ces.2020.116249.

[17] Hickel, S., Egerer, C. P., and Larsson, J., "Subgrid-scale modeling for implicit large eddy simulation of compressible flows and shock-turbulence interaction," *Physics of Fluids*, Vol. 26, No. 10, 2014, p. 106101.

[18] Sandham, N., Yao, Y., and Lawal, A., "Large-eddy simulation of transonic turbulent flow over a bump," *International Journal of Heat and Fluid Flow*, Vol. 24, No. 4, 2003, pp. 584–595.

[19] Borazjani, I., "A Sharp-Interface Immersed Boundary Method for Compressible Flows with Shock-Particle Interaction," *AIAA Journal*, Vol. In Press, 2020.

[20] Borazjani, I., "Fluid-structure interaction, immersed boundary-finite element method simulations of bio-prosthetic heart valves," *Computer Methods in Applied Mechanics and Engineering*, Vol. 257, No. 0, 2013, pp. 103–116.

[21] Asgharzadeh, H., and Borazjani, I., "A Newton–Krylov method with an approximate analytical Jacobian for implicit solution of Navier–Stokes equations on staggered overset-curvilinear grids with immersed boundaries," *Journal of Computational Physics*, Vol. 331, 2017, pp. 227–256.

[22] Akbarzadeh, A. M., and Borazjani, I., "Large eddy simulations of a turbulent channel flow with a deforming wall undergoing high steepness traveling waves," *Physics of Fluids*, Vol. 31, No. 12, 2019, p. 125107. https://doi.org/10.1063/1.5131268.

[23] Akbarzadeh, A. M., and Borazjani, I., "Reducing flow separation of an inclined plate via travelling waves," *Journal of Fluid Mechanics*, Vol. 880, 2019, pp. 831–863. https://doi.org/10.1017/jfm.2019.705.

[24] Akbarzadeh, A. M., and Borazjani, I., "Controlling Flow Separation on a Thick Airfoil Using Backward Traveling Waves," *AIAA Journal*, Vol. 58, No. 9, 2020, pp. 3799–3807. https://doi.org/10.2514/1.j059428.

[25] Asadi, H., Asgharzadeh, H., and Borazjani, I., "On the scaling of propagation of periodically generated vortex rings," *Journal of Fluid Mechanics*, Vol. 853, 2018, pp. 150–170.

[26] Ogunka, U. E., Daghooghi, M., Akbarzadeh, A. M., and Borazjani, I., "The Ground Effect in Anguilliform Swimming," *Biomimetics*, Vol. 5, No. 1, 2020, p. 9. https://doi.org/10.3390/biomimetics5010009.

[27] Vreman, B., Geurts, B., and Kuerten, H., "Subgrid-modelling in LES of compressible flow," *Applied scientific research*, Vol. 54, No. 3, 1995, pp. 191–203.

[28] Gilmanov, A., and Sotiropoulos, F., "A hybrid Cartesian/immersed boundary method for simulating flows with 3D, geometrically complex, moving bodies," *Journal of Computational Physics*, Vol. 207, No. 2, 2005, pp. 457 – 492. https://doi.org/https://doi.org/10.1016/j.jcp.2005.01.020, URL http://www.sciencedirect.com/science/article/pii/S0021999105000379.

[29] Bryson, A., and Gross, R., "Diffraction of strong shocks by cones, cylinders, and spheres," *Journal of Fluid Mechanics*, Vol. 10, No. 1, 1961, pp. 1–16.